Gelation transitions of colloidal systems with bridging attractions

Guangcui Yuan, Junhua Luo, Charles C. Han, and Yun Liu

Phys. Rev. E **94**, 040601 — Published 31 October 2016

DOI: 10.1103/PhysRevE.94.040601

Gelation transitions of colloidal systems with bridging attractions

Guangcui Yuan,[1,2,3]* Junhua Luo,[1] Charles C. Han[1]* and Yun Liu[2,4]*

[1]*Institute of Chemistry, Chinese Academy of Sciences, Beijing 100190, China;*

[2]*Center for Neutron Research, National Institute of Standards and Technology, Gaithersburg, Maryland 20899, USA;*

[3]*Department of Polymer Engineering, University of Akron, Akron, Ohio 44325, USA;*

[4]*Department of Chemical and Biomolecular Engineering, University of Delaware, Newark, Delaware 19716, USA.*

Abstract

The gelation transitions in a colloidal system, where there is a strong reversible attraction between small soft microgels and large hard spheres, is systematically investigated. Different from the other extreme case of the widely studied depletion attraction systems that are also two-component systems, the strong attraction between small solvent and large solute particles introduce bridging attractions between large solute particles. We conclusively demonstrate that the formation of physical gels at the intermediate volume fraction of our bridging attraction system follows more closely with the percolation line that is in stark contrast to what are observed in depletion attraction systems, where the gelation transition is related with the frustrated spinodal separation, not purely kinetic phenomenon. Our results introduce a different way to control gelation transition in spherical colloidal systems, and imply that people need to be prudent when generalizing the physical picture of the gelation transitions obtained from systems with different origins of effective attraction as the solvent molecule may play important roles.

Glass and gelation transitions are commonly observed for many systems in our everyday life such as polymers, metallic systems, cement, and paints. However, the physical mechanisms governing these transitions are far from clear and remain as intensively investigated scientific topics. Spherical colloidal systems with a short-ranged attraction have long been used as ideal model systems to investigate these transitions in the past several decades [1-7]. When the range of the attraction is small enough, it has been shown by experiments, theories and computer simulations that spherical colloidal systems at high concentrations can have glass transitions into either repulsive driven glass or attractive driven glass depending on the attraction strength [8, 9]. Mode-coupling theory (MCT) has been shown to explain the transitions in these colloidal systems successfully [9-11].

Comparing to glass transitions, gelation transitions of spherical colloidal systems usually happen at relatively low concentrations. Computer simulation results indicated that the gelation at the volume fraction less than the critical concentration, which is around 0.29 for the sticky hard sphere system [12, 13], should be driven by the frustrated gas-liquid separation [14]. Experiments on a depletion attraction system demonstrated that the gelation transitions at the volume fraction up to about 0.16 indeed follow the gas-liquid phase transition line [1]. This concept has been widely considered a general theory for the gelation transition for spherical colloidal systems with a short-ranged attraction [1, 15, 16].

Colloidal systems with the depletion attractions are two-component systems consisting of small solvent particle and large solute colloidal particles where there is no attraction between solvent and solute particles. However, there are a wide range of colloidal systems where the small solvent particles can be reversibly attracted to the surface of large solute particles, such as oppositely charged colloidal particle suspensions [17], and protein solutions with counterions with large valency [18]. The extension of the results from depletion attraction systems to these colloidal systems have not been carefully examined when the interaction of the solvent molecules with large solute particles changes. Therefore, it is very interesting and critically important to vary the attraction strength between the solvent and solute particles to investigate

the effect of the attraction on the gelation process.

Tuning the attractive interaction between the small solvent particle and large solute particles is very challenging and has not been widely studied until recently despite its importance [18-20]. In this paper, we have studied the gelation transitions of colloidal systems, in which there is a strong reversible attraction between small particles and large colloidal particles while the interaction between like particles is nearly a hard sphere interaction. Because of the strong attraction between small and large colloidal particle, the small particle can serve as a bridge to connect neighbouring large particles to introduce the bridging attraction. Both the bridging attraction and depletion attraction colloidal system are binary systems with large asymmetric size ratio between two types of particles. The key difference between these two systems is the interaction between the small and large particles. By systematically varying the attraction strength between small and large particles, a system can gradually change from a depletion attraction system to a bridging attraction system, which is the extreme case where the attraction between the small and large particles is very strong.

Surprisingly, by carefully checking the gelation transition of our bridging attraction colloidal system, we found that the introduction of the attraction between small and large particles moves the gelation transition line significantly away from the gas-liquid transition line at intermediate volume fraction that is completely different from the results of depletion attraction systems. Our results thus introduce a different approach to control the gelation boundary by systematically tuning the attraction strength between solvent and solute particles. These results also have a fundamental impact on the understanding of gelation transition phase diagrams. It implies that the gelation boundaries of these kinds of two-component systems is sensitive to the physics origins of the effective attraction between large colloidal particles. The effect of small solvent particles plays much bigger roles than that people previously thought.

The systems investigated in this paper consist of *large* hard polystyrene (PS) spheres (R = 9600 Å) and *small* soft poly (N-isopropylacrylamide) (PNIPAM) microgels (R_h = 1400 Å) in solvent. Here, R is the sphere radius determined by neutron scattering (BT5-USANS, NCNR), R_h is the hydrodynamic radius determined

by dynamic light scattering (ALV-5000F). The solvent is a buoyancy-matching mixture of H_2O and D_2O with equal volume to avoid the sedimentation of PS spheres. The PS spheres are stabilized in the solvent by a thin shell of covalent bonded poly(vinylpyrrolidone), which is a non-charged and water-soluble polymer. The preparation of the systems has been discussed in details previously [16, 20-22].

At a given volume fraction of large PS spheres (Φ_L), the PS spheres behave essentially as hard spheres in the absence of small microgels. PNIPAM microgels can be reversibly adsorbed to the surface of PS spheres as demonstrated previously [21, 22]. By gradually adding the microgels, the large spheres are connected to each other through the bridging of small particles. As it is shown both experimentally [16, 20 - 22] and theoretically [23, 24], adding small particles enhances the effective attraction strength between large particles until the attraction strength reaches a maximum value, after which adding more small particles slowly decrease the effective attraction strength. This is a general characteristic of a bridging attraction system.

This nontrivial dependence of the effective attraction strength between large particles on the small particle concentration results in a fundamental change of the aggregation and phase behavior of our systems compared with depletion attraction systems. Since PS particles are large enough, their aggregation behaviors at very small volume fraction were first investigated by a microscope as shown in Fig. 1a. At a small Φ_L (0.2% volume fraction), the large PS particles remain dispersed as individual particles before adding small microgels (the 1st image). Adding small particles increases the effective attraction strength quickly resulting in the formation of large aggregations (the 2nd image). Further increasing the volume fraction, Φ_S, of small microgels, the large particles become re-dispersed as shown in the 3rd image. This aggregation behaviour as a function of Φ_S, is consistent with the change of the effective attraction between large PS particles in a bridging attraction system, and can be qualitatively explained by two-component sticky hard sphere systems with Baxter's theory [23, 25].

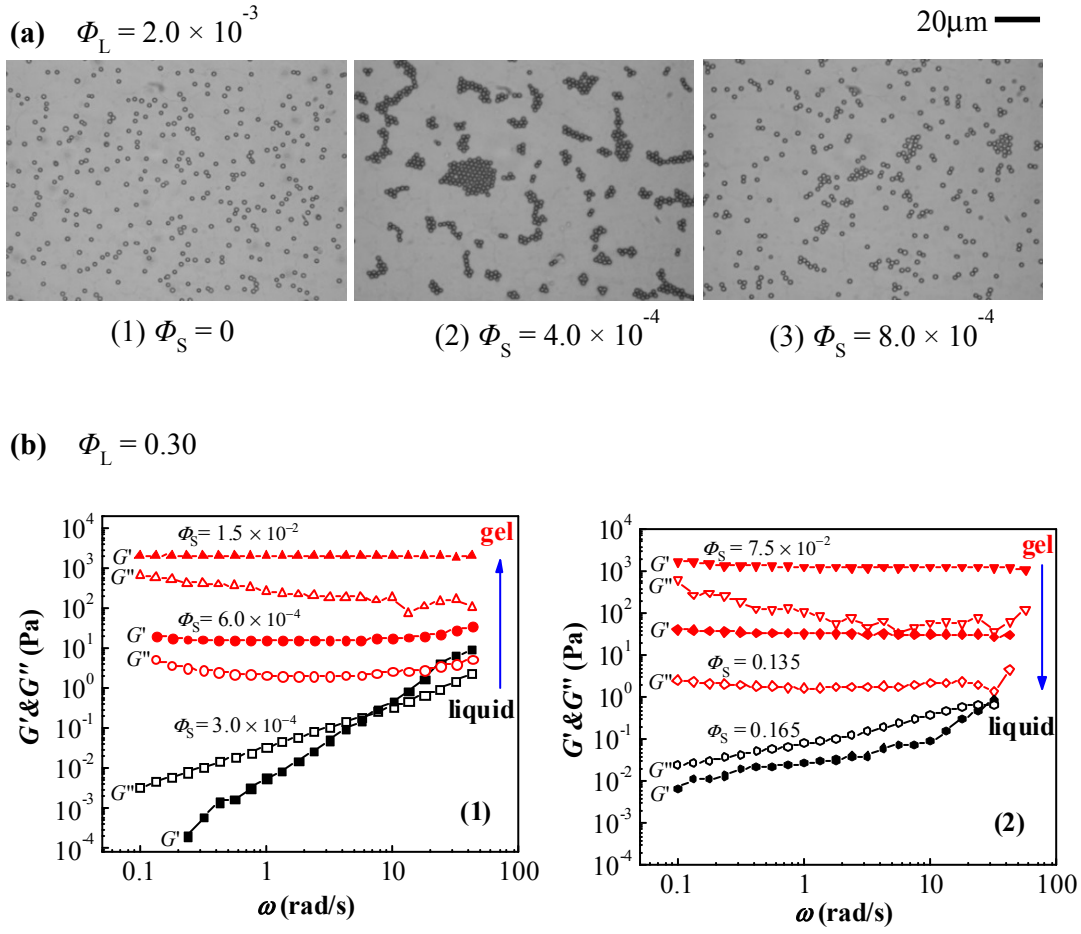

FIG. 1. (a) Optical microscopy images of dilute mixed suspensions with Φ_L = 2.0×10^{-3} at various Φ_S. Under the optical microscope, only the large PS spheres are visible because the microgel size is much smaller than the wavelength of visible light. (b) Frequency sweep data for concentrated mixed suspensions with Φ_L = 0.30 at various Φ_S. The stress amplitude is set to be σ= 0.1Pa .

When Φ_L is large, the size of the aggregates after adding small particles can be so large to form percolated clusters. The rheological responses of the samples are used to evaluate the transition from a liquid to a gel, and vice versa. At the gelation boundaries, the storage moduli, G', should be equal to the loss moduli, G'', for a wide range of frequency in small-amplitude oscillatory rheological measurements as shown

by Winter and Chambon [26]. In our experiments, at a given Φ_L, we have measured G' and G'' for $0.1 < \omega < 100$ rad/s for a series of samples by systematically increasing Φ_S. When G' is larger than G'' within the studied frequency range ($0.1 < \omega < 100$ rad/s), a sample is considered in gel states. If G' is smaller than G'', a sample is considered in a liquid state. It is also important to point out that the gel states in our sample are reversible physical gels. Its rheological properties can be consistently reproduced after breaking gels with a shearing force. (See the supporting information for rheological measurement details [27].) The gelation boundary is defined as the line separating the liquid state region to a gel state region.

When increasing Φ_S at a given Φ_L, a liquid-to-gel-to-liquid transition are observed for our samples. Fig. 1b shows G' (filled symbols) and G'' (open symbols) at $\Phi_L = 0.30$. Adding small particles can trigger a liquid-to-gel transition (the left panel in Fig. 1b), and the gel becomes stronger with increasing Φ_S. Black and red symbols correspond to liquid and gel state, respectively. The arrows in Fig. 1b indicate the direction of increasing Φ_S. The right panel of Fig. 1b indicates that up to a certain value, further increasing Φ_S gradually weakens the gel and leads to a gel-to-liquid transition. Therefore, at a given large particle concentration, Φ_L, there are two gelation transition concentrations for small particles. Adding small amount of small particles, the system can quickly become gel due to the increase of the effective attraction strength. When adding excessive amount of small particles, the gel samples become liquid again as the effective attraction strength decreases when Φ_S is too large.

The gelation transition boundaries are identified for suspensions with Φ_L ranging from 0.01 up to 0.35. The experimental phase diagram of liquid-gel-liquid transitions (diamonds) in the (Φ_L, Φ_S) plane is showed in Fig. 2. There are low-Φ_S gelation line and high-Φ_S gelation line. And these two lines meet around $\Phi_L \approx 0.03$ below which no gelation transitions are observed. The equilibrium phase diagram can be estimated using the binary sticky hard sphere systems based on the estimated interaction strength between the small and large particles [23]. If we assume that the individual

interaction between small and large particles (τ_{SL}) does not depend on the volume fraction of particles, the percolation lines (green stars), binodal lines (blue pluses), and spinodal lines (red circles) of our systems can be approximately estimated using the method proposed previously [23, 27]. Interestingly, the spinodal and binodal lines all form isolated islands. This is actually a general feature of this type of systems independent of the size of the particles [28]. Clearly, the experimental gel region occupies an open acute angle shape in the (Φ_L, Φ_S) plane and shows no trends to bend towards the gas-liquid transition lines with the volume fraction up to 0.35. Hence, the volume fraction dependence of the gelation transition boundary at the intermediate range volume fraction from 0.1 to 0.35 does not even qualitatively follow the equilibrium gas-liquid transition line. This is in stark contrast to the observations of the depletion attraction driven system where the gelation transition is believed to be driven by the frustrated gas-liquid transition. For the volume fraction less than 0.1, the gelation transition line agrees with the spinodal transition line consistent with the previous observation[16]. At this low concentration region, it is consistent with the picture observed previously in the depletion attraction system that the gelation is introduced by the frustrated spinodal transition [1, 14].

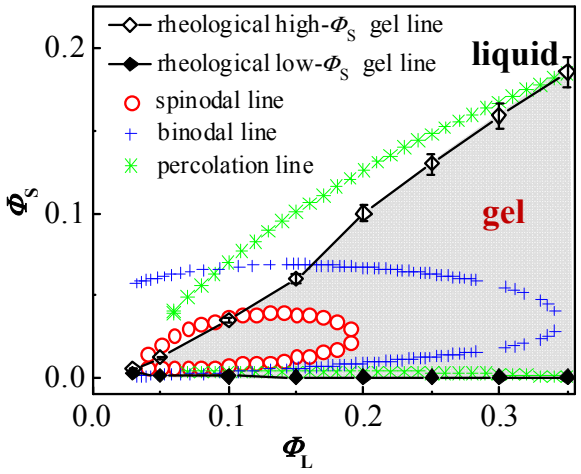

FIG. 2. Combination of rheological liquid-gel state diagram and theoretical phase diagram. Error bars was estimated by three independent measurements. The

theoretical phase diagram is obtained from data in Ref. 23 with diameter ratio $x = 0.14$ and stickiness parameter $\tau_{SL} = 0.012$.

As previously demonstrated that when the small particle size is small enough, the phase diagram of the large particles in this binary particle systems can be approximated by an equivalent one-component sticky hard sphere system where the effect of the small particles can be incorporated into the effective interaction between the large hard sphere systems [16]. Therefore, the phase diagram of the large colloidal particle can be considered as a sticky hard sphere system whose attraction strength depends now on Φ_S. We experimentally determined the effective attraction strength between the large colloidal particles, which is represented by the Baxter's stickiness parameter, τ, and compared our results with the literature results from other depletion attraction systems.

In order to determine the effective stickiness between large hard sphere systems, Ultra-small Angle Neutron Scattering (USANS) at the Center for Neutron Research in National Institute of Standards and Technology is used to measure the scattering patterns of the large spheres, where the contributions to the scattering patterns by small particles can be neglected. (The details of the instrument set-up and fitting method can be found in the supporting information [27].) Fig. 3a includes USANS patterns obtained from mixed suspensions around the gelation boundaries with fixed Φ_L at 0.30. The corresponding rheological property of these samples has been shown in Figs. 1b. Neutron scattering patterns are shifted vertically with each offset by a log $I = 1$ for clarity. Black and red symbols correspond to samples in liquid and gel states, respectively. Qualitatively judging from the trends of the intensity curves, a flat → upward → flat transitions of intensities approaching to the low q limit is consistent with rheological measurements, which shows a liquid-to-gel-to-liquid transitions with increasing Φ_S.

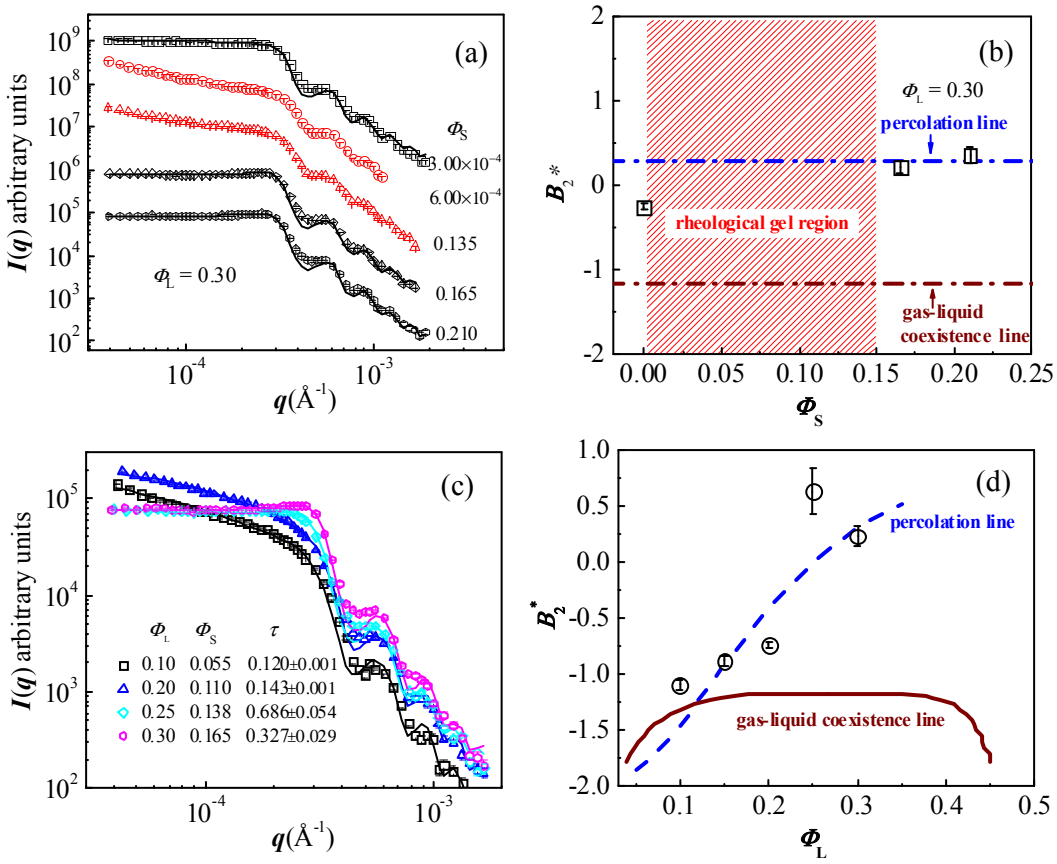

FIG. 3 Experimental (symbols) and fit (solid lines) intensity data scattered from suspensions: (a) fix volume fraction of large sphere Φ_L = 0.30 but vary volume fraction of small microgel Φ_S; (c) vary volume fraction of large sphere Φ_L but fix mixing ratio with Φ_S/Φ_L= 0.55. The (b) and (d) on the right are the reduced second virial coefficient B_2* corresponding to left (a) and (c), respectively. The blue and wine line in (b) indicate the theoretical percolation and phase separation values for Φ_L = 0.30, respectively. The blue dashed line and the wine solid line in (d) are the theoretical percolation line [29] and the gas-liquid coexistence line [12] for adhesive hard sphere system.

The USANS data are analyzed based on Baxter's one component sticky hard-sphere model after taking into account the instrument resolution. The effects caused by the small soft PNIPAM microgels are indirectly incorporated into their

influence on the effective interaction between the large hard PS microspheres. There are 7 parameters in the model: volume fraction (Φ_L), radius of sphere (R_g = 9600 Å), scattering length density (*SLD*) of sphere (1.4×10^{-6} Å^{-2}), *SLD* of solvent (2.8×10^{-6} Å^{-2}), perturbation parameter (ε), stickiness parameter (τ) and background. Only ε (which characterizes the range of attraction) and τ (which characterizes the overall attraction effect) are unconstrained variables in the fitting. All other parameters are pre-determined by fitting the scattering patterns from a dilute sample, at which the inter-particle structure factor can be considered unity. (See the supporting information for the details of the analysis method of neutron scattering data [27].) The analyzed τ value are represented by the reduced second virial coefficient B_2* with B_2* = 1-1/4τ. The fitting results for samples at liquid states are shown as solid lines in Fig. 3a.

The corresponding B_2* values are plotted in Fig. 3b showing the change of B_2* as a function of Φ_S at a fixed volume fraction of large particles (Φ_L = 0.3). As references, the blue horizontal line with B_2*= 0.30 corresponding to the estimated percolation value and one horizontal line with B_2*= -1.17 corresponding to the estimated gas-liquid phase separation line, are plotted too. Systems with B_2* < 0.30 are percolated systems for volume fraction Φ_L = 0.3 predicted by Baxter's model [29]. It is found that for liquid samples close to the gelation states, the corresponding B_2* is always close to the percolation, and far away from the gas-liquid transition line. It is noted that once in a gel state, the liquid theory is not valid to fit the data to obtain the correct effective attraction any more. However, from Fig. 3a, we can see that after crossing the gelation boundary (no matter for samples close to the low-Φ_S gelation line or the high-Φ_S gelation line) by adding more small particles, the scattering pattern has a big change at the low q.

Because the attraction strength changes much more slowly for Φ_S at high-Φ_S gelation line, it is thus much easier to control the effective attraction strength, τ, accurately at large Φ_S around its gelation transitions. In Fig. 3c, we have focused on the high-Φ_S gelation line and show the scattering profiles for mixtures with various Φ_L but with constant Φ_S/Φ_L = 0.55. The ratio chosen is based on the consideration that the rheological gel boundary on (Φ_L, Φ_S) plane (see Fig. 2) seems to follow a linear

relationship in the intermediate concentration region. The corresponding fitted parameters are mapped in the theoretical phase diagram of the adhesive hard sphere fluid (Fig. 3d). Our previous results indicate that when $\Phi_L < 0.1$, the gelation transition seems to follow the gas-liquid transition line [16]. However, the current results indicate that the formation of physical gel at intermediate volume fractions ($\Phi_L > 0.1$) follows more closely to the percolation line and deviate from the gas-liquid transition line. This result is consistent with the results obtained directly from the analysis of the binary system as shown in Fig. 2. It should be also noted that the USANS scattering patterns are very sensitive to the structure change of a system close to the gelation boundary. We have calculated the theoretical scattering patterns at different B_2* at $\Phi_L = 0.30$, which are shown in Fig. S3 in the supporting information [27]. The difference of the scattering patterns for B_2* at the percolation line and the gas-liquid separation line is so large that any possible uncertainties of the experimental B_2* introduced by the approximations built into our analysis model just cannot possibly move B_2* at the gelation transition boundary close to the gas liquid transition line at the intermediate range volume fraction. Hence, there is no any doubt that the gelation transition is closer to the percolation line and far away from the gas-liquid transition line.

In summary, we conclusively demonstrate that in bridging attraction systems, the physical mechanisms of gelation transitions at the intermediate range volume fraction are clearly different from the depletion systems. In general, both depletion attraction and bridging attraction systems are two extreme cases of binary colloidal systems with large asymmetric size ratio. In depletion attraction systems, the gelation transition is generally believed to be related with only thermodynamic equilibrium gas-liquid separation (frustrated spinodal separation), not purely kinetic phenomenon. Hence, the gelation transition should follow the equilibrium gas-liquid transition line in the depletion attraction driven systems. However, analysis of our results using both the two-component theory and one-component theory all indicate that the gelation transition is determined mostly by the percolation, not the gas-liquid transition at the intermediate range volume fraction. It is then reasonable to consider that the driven

mechanisms of gelation transitions for this kind of binary systems can transition from one mechanism to another one by varying the attraction strength between solvent and solute particles. Thus, we need to be prudent when generalizing the results obtained from the depletion attraction systems to other colloidal systems at the intermediate range volume fraction. Very interestingly, our results also indicate that we can control the gelation boundary by tuning the attraction strength between small and large colloidal particles. The effect of solvent molecules can play an important role in determining the gelation boundary.

There are many colloidal systems whose attraction strengths between the solute and solvent particles fall right in between depletion attraction and bridging attraction systems. By changing the attraction strength between solvent and solute particles, it might be possible that for some cases, both kinetic effect and the frustrated liquid-gas separation play equally important roles at different stages of the gelation transition, which need more future investigations. It is noted that a recent experiment on spherical silica systems showed also that the gelation transitions in a spherical silica particle systems follow the rigidity percolation line[30, 31], and is completely different from the gas-liquid separation lines where the effective attraction force between colloidal particles are based on interdigitated polymers [30]. The difference and similarity of this silica system and our binary colloidal system needs to be investigated in future.

This work is supported by the Chinese National Science Foundation (Project 21474121) and the National Basic Research Program of China (973 Program, 2012CB821503). This manuscript was prepared under the partial support of the cooperative agreements 70NANB12H239 and 70NANB10H256 from NIST, U.S. Department of Commerce. This work utilized facilities supported in part by the National Science Foundation under Agreement No. DMR-1508249. Certain commercial equipment, instruments, or materials (or suppliers, or software…) are identified in this paper to foster understanding. Such identification does not imply recommendation or endorsement by the U.S. National Institute of Standards and

Technology, nor does it imply that the materials or equipment identified are necessarily the best available for the purpose.

* Correspond authors: yunliu@nist.gov, guangcui.yuan@nist.gov, and c.c.han@iccas.ac.cn

1. P. J. Lu, E. Zaccarelli, F. Ciulla, A. B. Schofield, F. Sciortino and D. A. Weitz, Nature, **453**, 499 (2008).
2. W. C. K. Poon, A. D. Pirie, M. D. Haw and P. N. Pusey, Physica A **235**, 110 (1997).
3. H. Tanaka, Y. Nishikawa and T. Koyama, J. Phys.: Condens. Matter **17**, L143 (2005).
4. P. Bartlett, R. H. Ottewill, and P. N. Pusey, J. Chem. Phys. **93**, 1299 (1990).
5. M. A. Miller and D. Frenkel, Phys. Rev. Lett. **90**, 135702 (2003).
6. E. Zaccarelli, J. Phys.: Condens. Matter **19**, 323101 (2007).
7. F. Sciortino, S. Mossa, E. Zaccarelli and P. Tartaglia, Phys. Rev. Lett. **93**, 055701 (2004).
8. K. N. Pham, A. M. Puertas, J. Bergenholtz, S. U. Egelhaff, A. Moussaïd, P. N. Pusey, A. B. Schofield, M. E. Cates, M. Fuchs, W. C. K. Poon, Science **296**, 104 (2002).
9. K. A. Dawson, G. Foffi, M. Fuchs, W. Götze, F. Sciortino, M. Sperl, P. Tartaglia, Th. Voigtmann and E. Zaccarelli, Phys. Rev. E **63**, 011401 (2000).
10. L. Fabbian, W. Götze, F. Sciortino, P. Tartaglia and F. Thiery, Phys. Rev. E **59**, 1347 (1999).
11. K. A. Dawson, Curr. Opin. Colloid Interface Sci. **7**, 218 (2002).
12. M. A. Miller and D. Frenkel, J. Chem. Phys. **121**, 535 (2004).
13. J. Largo, M. A. Miller, F.Sciortino, J. Chem. Phys. **128**, 134513(2008)
14. G. Foffi, C. De Michele, F. Sciortino and P. Tartaglia, Phys. Rev. Lett. **94**, 078301 (2005).

15. F. Cardinaux, T. Gibaud, A. Stradner and P. Schurtenberger, Phys. Rev. Lett. **99**, 118301 (2007).
16. J. Luo, G. Yuan, C. Zhao, C. C. Han, J. Chen and Y. Liu, Soft Matter **11**, 2494 (2015).
17. J. F. Gilchrist, A. T. Chan, E. R. Weeks and J. A. Lewis, Langmuir **21**, 11040 (2005).
18. F. Roosen-Runge, F. Zhang, F. Schreiber and R. Roth, Sci. Rep. **4**, 7016 (2014).
19. B. Bharti, J. Meissner, S. H. L. Klapp and G. H. Findenegg, Soft Matter **10**, 718 (2014).
20. C. Zhao, G. Yuan and C. C. Han, Soft Matter **10**, 8905 (2014).
21. C. Zhao, G. Yuan, D. Jia and C. C. Han, Soft Matter **8**, 7036 (2012).
22. C. Zhao, G. Yuan and C. C. Han, Macromolecules **45**, 9468 (2012).
23. J. Chen, S. R. Kline and Y. Liu, J. Chem. Phys. **142**, 084904 (2015).
24. R. Fantoni, A. Giacometi and A. Santos, J. Chem. Phys. **142**, 224905 (2015).
25. R. J. Baxter, J. Chem. Phys. **49**, 2770 (1968).
26. H. H. Winter and F. Chambon, J. Rheol. **30**, 367 (1986).
27. See supplementary material at [*URL will be inserted by publisher*] for some details of rheological measurement, USANS measurement/fitting, and theoretical calculation of the equilibrium phase diagram.
28. J. Chen, S. R. Kline and Y. Liu, J. Phys.: Condens. Matter **28**, 455102 (2016).
29. H. Verduin and J. K. G. Dhont, J. Colloid Interface Sci. **172**, 425 (1995).
30. A. P. R. Eberle, N. J. Wagner and R. Castañeda-Priego, Phys. Rev. Lett. **106**, 105704 (2011).
31. N. E. Valdez-Pérez, Y. Liu, A. P. R. Eberle, N. J. Wagner, R. Castañeda-Priego, Phys. Rev. E **88**, 060302 (2013)